PROCEEDINGS OF SCIENCE

R-process Experimental Campaign at the National Superconducting Cyclotron Laboratory

Jorge Pereira[*1,2], **Ana Becerril**[1,2], **Thom Elliot**[1,2], **Alfredo Estrade**[1,2,3], **Daniel Galaviz**[1,2], **Linda Kern**[1,2], **G. Lorusso**[1,2,3], **Paul Mantica**[1,4], **Milan Matos**[1,2], **Fernando Montes**[1,2,3], **Hendrik Schatz**[1,2,3]

1) National Superconducting Cyclotron Laboratory (NSCL),
2) Joint Institute of Nuclear Astrophysics (JINA),
3) Department of Physics and Astronomy,
4) Department of Chemistry
Michigan State University (East Lansing) Michigan, USA
E-mail: pereira@nscl.msu.edu

Stefan Hennrich[1,2], **Karl-Ludwig Kratz**[1,2], **Oliver Arndt**[1,2], **Ruben Kessler**[1,2], **Florian Schertz**[1,2], **Bernd Pfeiffer**[1,2]

1) Institut für Kernchemie,
2) Virtuelles Institut für Struktur der Kerne and Nuklearer Astrophysik (VISTARS)
Johannes Gutenberg, Universität Mainz (Mainz) Germany

M. Quinn[1,2], **A. Aprahamian**[1,2], **A. Woehr**[1,2]

1) Institute of Structure and Nuclear Astrophysics,
2) Joint Institute of Nuclear Astrophysics (JINA)
University of Notre Dame (South Bend) Indiana, USA

Ed Smith[1,2]

1) Department of Physics
Ohio State University (Columbus) Ohio, USA,
2) Joint Institute of Nuclear Astrophysics (JINA)
Michigan State University (East Lansing) Michigan, USA

William Walters

Department of Chemistry and Biochemistry
University of Maryland (College Park) Maryland, USA

International Symposium on Nuclear Astrophysics – Nuclei in the Cosmos – IX
CERN, Geneva, Switzerland
25-30 June, 2006

[*] Speaker

A JINA/VISTARS r-process campaign was completed at the A1900 Fragment Separator of the National Superconducting Cyclotron Laboratory in the fall of 2005. The purpose of the campaign was the measurement of the β-decay half-lives and β-delayed neutron-emission probabilities of different unknown neutron-rich nuclei participating in the r-process. From these observables it will be possible to extract information about the region between the N=56 sub-shell closure and the *sudden onset of deformation* at N=60 in the A≈100 region, and the "new shell structures" around the possible local, spherical double sub-shell closure at Z=40, N=70, which may help clarify the origin of the calculated r-process abundance deficiencies around A=110. Moreover, the region of the chart of nuclides investigated in the campaign included some important r-process *waiting-points* nuclei, whose β-decay properties are crucial for understanding the r-process abundance pattern. Details of this campaign will be presented, emphasizing the experimental challenges that had to be faced.

1. Introduction

Nucleosynthesis in the r-process constitutes one of the most exciting and challenging open questions in nuclear astrophysics. In particular, the astrophysical scenario where this process occurs has not yet been identified (for a general review see for instance Ref.[1]). Models aimed to reproduce the observed r-process abundances are sensitive to both the astrophysical conditions associated with the assumed scenario and the nuclear properties of the very neutron-rich nuclei involved in the process. In classical r-process models–where equilibrium between neutron-capture and photo-neutron disintegration holds–there are two important nuclear properties with significant impact in the calculated abundances: the masses of nuclei near the neutron drip line, defining the "path" along which the r-process flow of matter is built up, and the β-decay properties, in particular the β-decay half-lives and β-delayed neutron-emission probabilities, which play a crucial role in determining the abundance pattern prior and after freeze-out, respectively. The fact that many of the r-process nuclei are extremely exotic–and therefore difficult to produce–makes their measurement very difficult and in many cases impossible with the current experimental facilities. As a matter of fact, astrophysical r-process models have to rely on theoretical estimates of nuclear masses and β-decay properties of nuclei near the neutron drip line, where very little is known. This questions to what extend nuclear structure of nuclei involved in the r-process can be deduced from our understanding of nuclei closer to stability.

1.1 Sensitivity of r-process models to nuclear structure

A comprehensive theoretical and experimental knowledge of the structure of nuclei far away from stability is mandatory in order to fix the astrophysical properties of the r-process scenario(s). An illustrative example of the dichotomy Astrophysics vs. Nuclear Physics is found in the region prior to the A=130 abundance peak, where r-process models tend to underestimate the productions by an order of magnitude or more. On one

hand, it is claimed that the lower part of the A=130 abundance peak is sensitive to neutrino post-processing effects [2]. On the other hand, it has been demonstrated that this region is very sensitive to the details of the structure of the corresponding r-process nuclei; in particular, it has been shown that the underproduction of abundances can be largely corrected if one assumes a reduction or *quenching* of the N=82 shell gap far from stability [3] (see Fig.1 and Refs.[4,5]). Therefore, disparities between r-process model calculations with observed abundances provide unique insight about the neutrino flux during the r-process, once the underlying nuclear structure is understood.

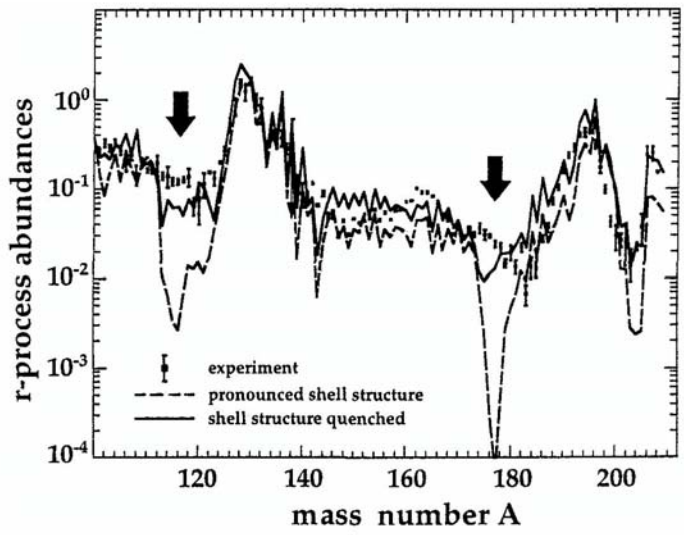

Fig.1: *Global r-abundance fits for the ETFSI-I mass model [4] with pronounced shell structure below ^{132}Sn and the ETFSI-Q formula [5] with quenched N=82 and N=126 shell gaps.*

1.2 R-process motivations

The motivation of the present campaign was the study of nuclear structure in two different interesting regions in the r-process:

i) A first experiment, was focused on the N≥54 Ge to Br isotopes, which can constitute part of the N>50 neutron-rich seed nuclear composition after α-rich freeze-out, in the hot-bubble neutrino-wind scenario [6]. From a nuclear-structure point of view, these nuclei lie in the region between the N=56 sub-shell closure and the *sudden onset of deformation* at N=60, south of the range Sr-Zr, for which the most pronounced transition from spherical to strongly deformed ground-state shapes has been observed. Assuming ^{78}Ni acts as an inner core, this region of nuclei lies below the minimum four valence proton-pairs and five valence neutron-pairs required for observing a *sudden onset of deformation* [7]. The study of the nuclear-shape evolution for these nuclei can thus provide insight into the pn-interaction amongst the valence nucleons outside the doubly-magic spherical ^{78}Ni. Once these nuclear properties are better understood, it will

be possible to obtain a better interpretation of the "under-abundances" (compared to the Solar System) observed in ultra-metal poor halo stars for the main r-process, and define more restrictive constraints on the stellar conditions for the secondary *weak* r-process [3].

ii) A second experiment was focused on the nuclear structure of A≈110 r-process nuclei. Besides the shape evolution from the sub-shell N=56 to the *sudden onset of deformation* at N=60, the region of the refractory elements around Zr beyond N≈66 should contain another phase transition from strongly prolate, oblate or triaxial shapes to spherical neutron magicity at N=82. Self-consistent HFB calculations of the potential-energy surface (PES) of neutron-rich Zr isotopes [8,9], however, have shown that the tetrahedral minimum in the PES of ^{110}Zr and ^{112}Zr may lie lower than their secondary prolate minimum. The experimental observation of this possible local spherical "tetrahedral magic gap" at N=70 would have strong consequences in the understanding of the r-process, as it may be an indirect signature of the N=82 *shell quenching*. Therefore, the experimental study of nuclei in this region can provide insight into the question of the abundance trough prior to the A=130 peak, predicted by r-process model calculations.

1.3 Experimental observables measured during the campaign

The experimental observables measured in the completed experiments were the β-decay half-lives and β-delayed neutron-emission probabilities of nuclei in the two regions described above. These particular observables were chosen since:

i) They are direct inputs in r-process model calculations, which will substitute theoretical estimates.

ii) Because these two experiments deal with the degree of deformation of neutron-rich nuclei in the r-process, a first hint about the shape of a nucleus can already come from the measurement of the β-decay half-life ($T_{1/2}$) and the β-delayed neutron-emission probability (P_n). Within the concept of the β-strength function $S_\beta(E)$, half-lives are dominated by the lowest energy part of $S_\beta(E)$, while P_n-values are sensitive to the β-feeding to the energy region just above the neutron separation energy. The sensitivity of these quantities to the different parts of $S_\beta(E)$ is governed by the strong energy dependence of the Fermi function, $(Q_\beta\text{-}E)^5$; as the shape of the β-strength function depends on nuclear structure, so do the values of $T_{1/2}$ and P_n. As an example, we show on the right and left side of Fig.2, the possible changes in the β-decay pattern of ^{110}Zr. According to present model predictions (e.g. the "un-quenched" FRDM [10]), this nucleus is strongly deformed in its ground state. Hence, the deformed QRPA [11] predicts β-decay to a multitude of narrow-spaced 1^+ levels in the deformed daughter ^{110}Nb, with the strongest GT-branch to a level at about 1.67MeV. This decay pattern results in a $T_{1/2}$≈88msec and a P_n≈8%. On the other hand, when assuming a strongly "quenched" N=82 shell, ^{110}Zr will be much less deformed or even become a (near-) spherical, doubly semi-magic nucleus. In this case, the corresponding GT-decay pattern would change drastically, and the resulting gross β-decay properties would be

completely dominated by a single allowed transition to a 1^+ state at about 1.13MeV in ^{110}Nb. The $T_{1/2}$ would become shorter by about a factor 6, and the P_n value would be smaller by about a factor 11.

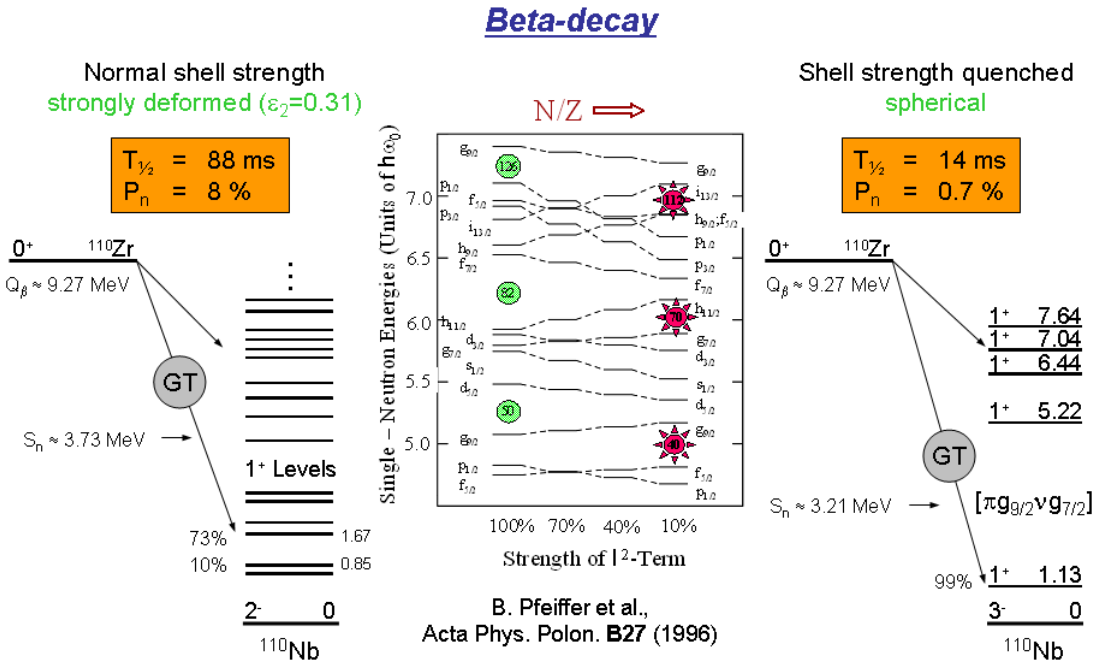

Fig. 2: *Possible β-decay properties of ^{110}Zr. The left part shows our QRPA predictions for GT-decay of a strongly deformed ^{110}Zr - ^{110}Nb system, as expected from the "unquenched" FRDM with the classical neutron shell gaps [10]. The right part shows the GT-decay when assuming ^{110}Zr to be a spherical, doubly semi-magic nucleus with "quenched" shells [11]. In the middle part of the figure, the SP-energies for neutrons in a "classical" Nilsson potential (left part) and in a well where the l^2-term (the parameter μ_n) is reduced gradually to one-tenth of the standard value (right part).*

iii) The conditions for measuring β-decay half-lives and P_n-values are generally less restrictive in terms of beam intensities than gamma-decay studies. Therefore, it is possible to study nuclei further away from stability.

2. Experiments

The campaign was performed at the National Superconducting Cyclotron Laboratory (NSCL) at Michigan State University (MSU). Figure 3 shows a layout of the NSCL with its experimental facilities. The two coupled cyclotrons (K500 + K1200), at the beginning of the beam line, accelerated a ^{136}Xe primary beam up to 120MeV/u. This beam was then sent onto a 242mg/cm^2 Be target located at the entrance of the A1900 in-flight separator. The nuclei investigated in each of the two experiments were produced by fragmentation of the ^{136}Xe beam by beryllium nuclei. Due to momentum

conservation, the reaction products were forward-emitted into the A1900. A specially-designed achromatic Al wedge, mounted in the dispersive focal plane, combined with the optics of the A1900, allowed a spatial separation of the nuclei transmitted to the final focal plane according to their different energy losses and magnetic rigidities. Two position-sensitive plastic scintillators at the intermediate (dispersive) and final (achromatic) focal planes were used to measure the time-of-flight (ToF) of the transmitted nuclei, as well as to correct the intrinsic dependence of this time-of-flight with their transversal position at the dispersive focal plane. Once separated, the nuclei were guided into the final experimental area, equipped with an implantation setup, designed to measure β-decay half-lives and β-delayed neutron-emission probabilities of the implanted nuclei. By combining the energy-loss signals (ΔE), measured with a Si detector at the experimental area, with the ToF signal along the A1900, it was possible to separate unambiguously the different nuclear species coming in the same cocktail. Figure 4 shows the so-called particle-ID matrix (particle-identification matrix), where each blob corresponds to a different combination of proton and neutron numbers.

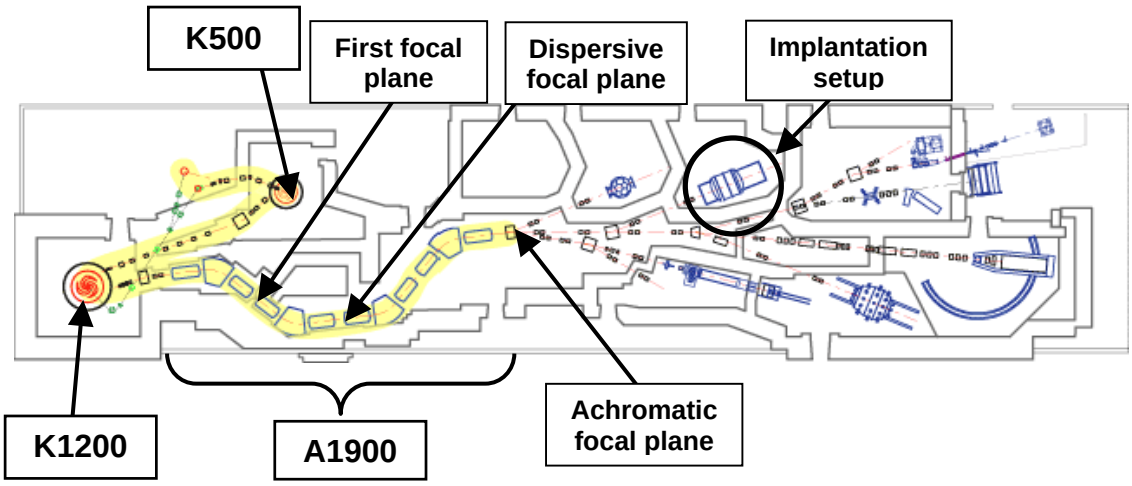

Fig.3: *Layout of the NSCL with the main experimental devices used in the campaign.*

2.1 Detector setup

The detection setup is shown in Fig.5. In the first part of the experiment (around 8 hours of beam time) known microsecond isomers were implanted in a 4mm Al degrader surrounded by three Segmented Germanium Array (SeGA) detectors [12], symmetrically mounted around the beam axis (see Fig.6). A Si PIN detector upstream was used to measure the energy-loss signal, which, combined with the ToF signal, provided the particle-ID matrix. This detector gave also the trigger that opened a common gate for a group of Ortec ADCs and the start signal for a group of Phillips TDCs associated with the Ge detectors.

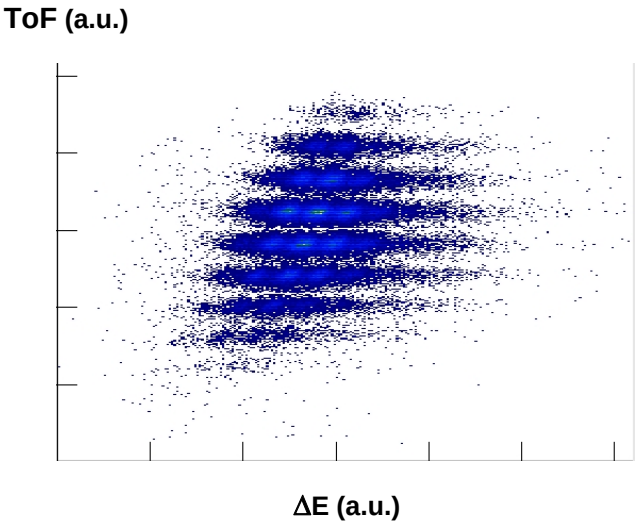

Fig. 4: *Particle-ID matrix (Particle-identification matrix) obtained during one of the experiments. Each blob corresponds to different nuclear species.*

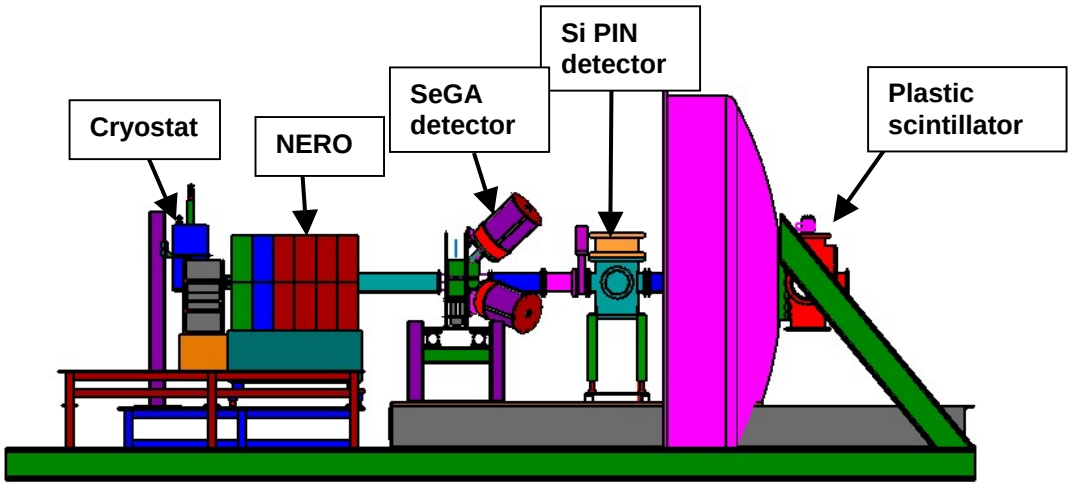

Fig.5*: Implantation setup mounted in the experimental area downstream the A1900. Shown are the three SeGA detectors and the NERO + BCS implantation system (see text for details).*

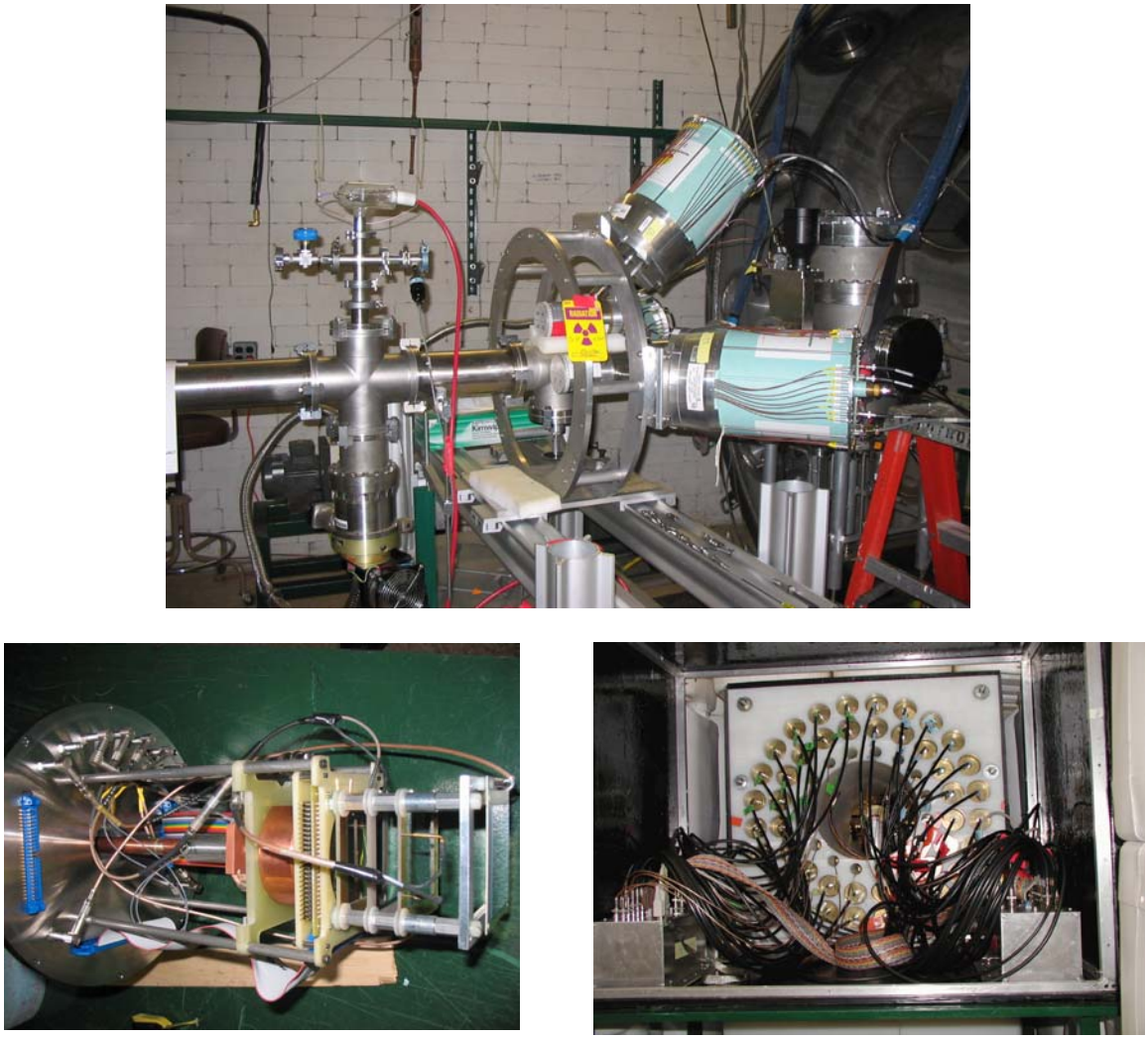

Fig.6: *Upper panel: particle-ID setup. Shown are the three SeGA detectors around the Al implantation degrader. Lower panels: implantation setup. Left panel: Beta Counting System (BCS). Right panel: Neutron Emission Ratio Observer (NERO) detector. The BCS chamber is located in the center hole of the polyethylene matrix.*

The Beta Counting System (BCS) [13] was placed downstream of the gamma-ID station. It consisted of a stack of four Si PIN detectors, used to measure the energy-loss of the exotic species, followed by a doubly-segmented 40×40 Si strip detector (DSSD), where the nuclei were implanted. A final single-segmented 16 Si strip detector (SSSD) was used to veto light particles and nuclei that punch-through the implantation detector. Finally, a Ge crystal mounted downstream was tested for spectroscopic purposes. Figure 6 shows the implantation setup used during the campaign.

The BCS was surrounded by the Neutron Emission Ratio Observer (NERO) detector [14] (see Fig.6) which was used to measure β-delayed neutrons. This detector consisted of 16 ^{3}He and 44 B_3F proportional counter tubes embedded in a polyethylene matrix used to thermalize the emitted neutrons.

Signals from each PIN detector went through a sequence of TC148 preamplifier and TC428 shaper/amplifier that ended in a VME CAEN V785 ADC. The fast output of the amplifier went to a TC455 CFD that provided the required signals for the logic. Both the DSSD and SSSD detector signals went into a group of special CPA16 Multichannel Systems preamplifiers that provided high- and low-gain outputs. The low-gain output, carrying information about the energy of the implanted nuclei, fed a group of VME CAEN V785 ADC, while the high-gain output, generated by decay events, went into a double shaper/discriminator Pico-system module. Outputs from the discriminators were used for logic purposes, while the analogic shaper outputs went directly into a group of CAEN VME V785 ADCs.

Concerning the NERO detector, the signals of the different proportional counters were grouped in four quadrants and sent into four different preamplifiers used for each quadrant. Signals went then into a double shaper/discriminator Pico-system module. Outputs from the discriminator fed a group of scalers and a special VME CAEN V766 TDC of 80msec range used to measure the neutron multiplicities associated with each β-decay event. The analogic output signals from the shapers were sent into a group of VME CAEN V785 ADCs.

Finally, a coincidence register VME unit SIS3600 was used in order to speed the readout of a total of about 300 channels.

2.2 Experimental challenges

During the preparation of the campaign, there were three important experimental challenges that had to be faced:

i) The extremely low production rates

During the preparation of the experiment, production rates of the nuclei of interest were calculated with the program LISE [15], which accounts for the losses due to the limited acceptance of the A1900 and beam lines. Fragmentation cross-sections were calculated with the EPAX program [16]. While this semi-phenomenological parameterization provides very accurate values for nuclei relatively close to stability, it was found –by comparing the calculated productions with values measured in previous experiments– that the calculated cross-sections were overestimated in some cases by up to three orders of magnitude. This makes the production of r-process nuclei challenging. Nevertheless, with the very high primary-beam intensities provided by the CCF, it was possible to reach the r-process path in this region at the limit of 20 implantations per week. This is just in the limit of required statistics to extract half-life information.

ii) The presence of primary-beam charge-states in the cocktail beam

In the first half of the A1900, from the target station to the dispersive focal plane, the nuclei are spatially separated according to their magnetic rigidity. Apart from the desired nuclei, any species with magnetic rigidities within the ±2.5% acceptance is transmitted, thus contaminating the cocktail of nuclei. Because the nuclei of interest are on the neutron-rich side, some of the contaminants included charge-states from the primary beam. In particular, $^{136}Xe^{+50,+51,+52}$ and $^{136}Xe^{+49,+50,+51}$ were transmitted on each of the two experiments, respectively. Therefore, in order to avoid any damage of our

detectors (especially the plastic scintillator at the dispersive focal plane) due to the very high intensities of these contaminants, it was necessary to block these contaminants. For this purpose, a beam blocking system was designed and mounted at the first focal plane consisting of two tungsten slits, on the left and right sides and a "finger" located in the middle of the beam axis. Each of these elements blocked one of the three primary-beam charge-state contaminants, leaving two gaps in between.

iii) Particle ID

In order to tag the different blobs displayed in the particle-ID matrix, it was necessary to have some known nuclei included in the cocktail, so that transmitted species could be identified according to their positions in the particle-ID matrix with respect to the nuclei of reference. The references used in both experiments were a set of microsecond isomers with known gamma decay lines. By detecting these gamma lines in coincidence with the implanted nuclei it was possible to identify these microsecond isomers within the cocktail. This technique set additional technical constraints because it was necessary to fit, in the same A1900 setting, the rather different magnetic rigidities of the microsecond isomers and the nuclei of interest. With the blocking system used in the experiments, microsecond isomers passed through the gap corresponding to the lower magnetic rigidities (less exotic species), whereas the nuclei of interest were transmitted through the high magnetic-rigidity gap.

Gamma decay lines measured with the Ge array were gated on the different blobs shown in the particle-ID matrix (see Fig.4). Several known microsecond isomers were identified [17,18]:

^{121}Pd (135keV), ^{123}Ag (714keV), ^{124}Ag (156keV), ^{125}Ag (685keV),
^{125}Cd (720keV, 743keV), ^{98}Y (120.9keV, 170.3keV)

Figure 7 shows the particle-ID matrices obtained from the measured microsecond isomers in each experiment. Blobs on the left side of the line correspond to nuclei involved in the r-process.

3. Analysis

i) β-decay half-lives

In order to separate implantation, decay and background events specific conditions were assigned to each of them. When a signal was registered in the first Si detector and in the low-gain output from the two sides of the DSSD, the event was considered to to be an implantation. A decay event was assumed when there is a coincidence between no-signal in the first Si detector and high-gain output signals from each side of the DSSD. When an implantation event is measured, the time –recorded from a 50MHz VME SIS3820 clock– and the pixel at which the event was implanted were recorded. If a consecutive decay event occurs in the same pixel within a time gate of 10 seconds, then the event is associated with the previous implantation event and its time is registered too. By distributing the time differences between implantation and decay events

associated with a given nucleus, we could produce a decay-curve. Figure 8 shows the preliminary decay-curve obtained online for ^{105}Zr.

Multi-parameter fits including background and decay-event curves from mother, daughter and granddaughter nuclei are currently being calculated to extract the final half-lives.

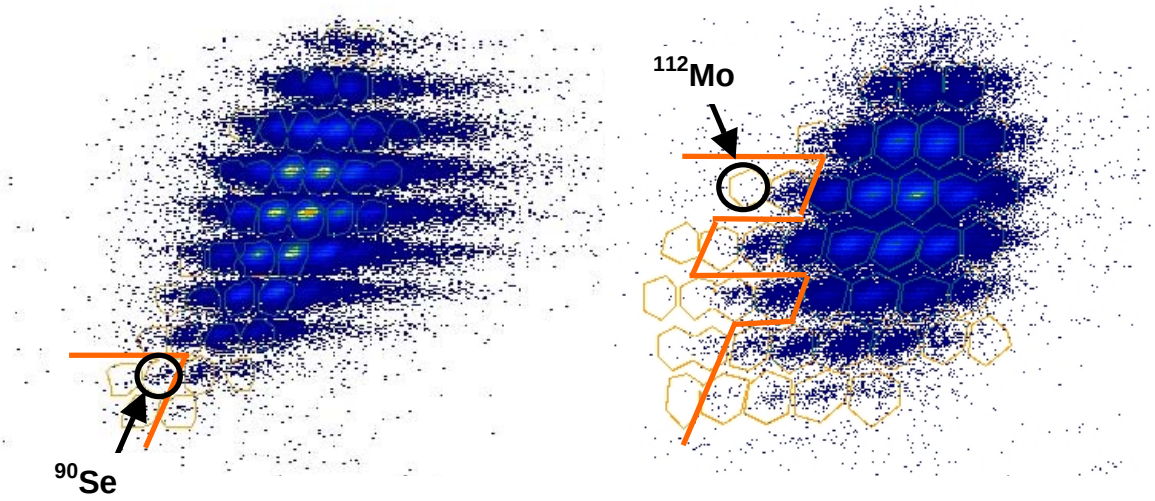

Fig.7: *Particle-ID matrices obtained for each experiment. Blobs on the left side of the line correspond to nuclei involved in the r-process whose β-decay properties will be determined from the analysis of the experiments.*

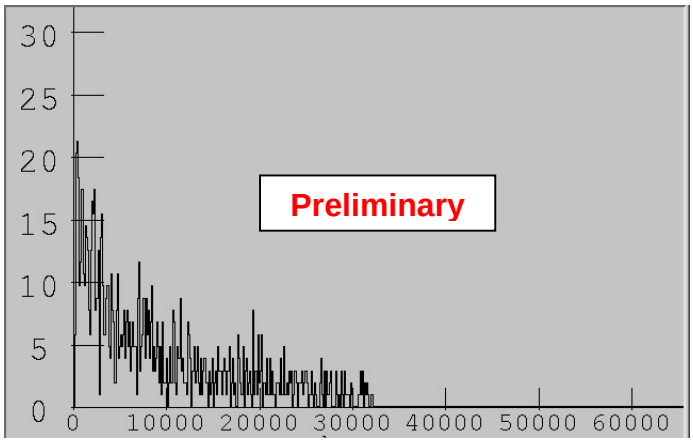

Fig.8: *β-decay curve of ^{105}Zr measured during one of the experiments.*

ii) β-delayed neutron-emission probabilities

After a decay event was identified, a gate of 200μsec was opened in order to search for possible correlated delayed neutrons. This time window was calculated on the basis of the time needed by the emitted neutrons to be thermalized in the polyethylene matrix before being detected in one of the proportional counters. The CAEN V766 TDC has multi-hit capabilities, allowing the detection of multiple neutron events associated with a single β-decay. By grouping the neutron events according to their multiplicities and normalizing them to the total number of β-decay associated with the corresponding decaying nucleus, we can then extract the P_n-value.

The data analysis is currently being done in collaboration between the National Superconducting Cyclotron Laboratory (Michigan), the University of Notre Dame (Indiana) and the University of Mainz (Germany).

4. Summary

An r-process motivated experimental campaign was carried out at the National Superconducting Cyclotron Laboratory. The goal of the campaign was to investigate the shape-evolution of nuclei far away from stability that are involved in the r-process. The probes used for such studies were the β-decay half-lives and P_n-values, which are particularly sensitive to the structure of the decaying nuclei at different energies through the β-strength function. Results obtained from the data analysis will provide insight into relevant questions about nuclear structure of exotic nuclei including *shell quenching* and pn-interactions between exotic combinations of valence nucleons. The knowledge gained from this analysis in terms of nuclear structure will put r-process models on a more solid basis, in order to investigate the astrophysical conditions that might affect the synthesis of heavy elements. The measured β-decay properties will also provide direct inputs needed in r-process model calculations.

The performance of the detection setup, including a special blocking system designed to remove primary-beam charge-state contaminants from the cocktail beam, demonstrated the capabilities of the NSCL to perform β-decay studies of extremely neutron-rich r-process nuclei. Results from previous β-decay experiments have been already published (see e.g. Refs. [19-23]. Moreover, new techniques to measure masses of neutron-rich nuclei have being recently tested [24], making the NSCL to be one of the prime facilities to perform this type of r-process experiments. Future next generation facilities (e.g. NSCL upgrade) will be necessary to cover unknown r-process regions, in order to solve at last and at once one of the most intriguing questions of Nature, namely, the origin of the heavy elements [25].

References

[1] J. J. Cowan and F.-K. Thielemann, Phys. Today (October 2004) 47

[2] Y.-Z. Qian et al., Phys. Rev. C55 (1997) 1532

[3] B. Pfeiffer et al. Z.Physik A357 (1997) 235

[4] Y. Aboussir et al., ADNDT 61 (1995) 127

[5] J.M. Pearson et al., Phys. Lett. B387 (1996) 455

[6] Y.-Z. Qian and S.E.Woosley, Ap. J. 471 (1996) 331

[7] R.F. Casten, Nucl. Phys. A443 (1985) 1

[8] J. Dudek et al., Phys. Rev. Lett. 25 (2002) 252502

[9] N. Schunck et al., Phys. Rev. C69 (2004) 061305

[10] P. Möller at al., ADNDT 59 (1995) 185

[11] P. Möller et al., Phys. Rev. C67 (2003) 055802

[12] W.F. Mueller et al., Nucl. Instr. and Meth. A466 (2001) 492

[13] J.I. Prisciandaro et al., Nucl. Instr. and Meth. A505 (2003) 140

[14] G. Lorusso et al., proceeding of this conference

[15] O. Tarasov, http://groups.nscl.msu.edu/lise/7_5/lise++_7_5.pdf

[16] K. Summerer et al., Phys. Rev. C61 (2000) 034607

[17] G.Audi et al., Nucl. Phys. A729 (2003) 27

[18] B.E. Tomlin, PhD. Thesis, Michigan State University, 2006

[19] J.I. Prisciandaro et al., Phys. Lett. B510 (2001) 17

[20] P.F. Mantica et al., Phys. Rev. C67 (2003) 014311

[21] P.F. Mantica et al., Phys. Rev. C68 (2003) 044311

[22] P.Hosmer et al., Phys. Rev. Lett. 94 (2005) 112501

[23] F. Montes et al., Phys. Rev. C73 (2006) 035801

[24] A. Estrade et al., proceeding of this conference

[25] NAS report, “Connecting Quarks with the Cosmos: Eleven Science Questions for the New Century”